Dariusz CHABERSKI[1]

Nicolaus Copernicus University, Faculty of Physics, Astronomy and Informatics, 87-100 Toruń, Poland (1)

High-resolution time-interval generator

Abstract. The paper presents the design of a high-resolution TI (Time-Interval) generator implemented into FPGA (Field-Programmable-Gate-Array) Xilinx Virtex 5 device and obtained experimental test results. The improvement of resolution is realized by the use of a chain of DCDEs (Digitally-Controlled-Delay-Elements). The presented TI generator allows for generating either TIs of constant length or TIs of specified Gaussian distribution. Experimental results include TI histograms measured by the LeCroy 804Zi oscilloscope.

*Streszczenie. Artykuł przedstawia projekt wysokorozdzielczego generatora odcinków czasu zaimplementowanego w strukturze programowalnej FPGA Xilinx Virtex 5 wraz z wynikami eksperymentalnymi uzyskanymi z wykorzystaniem oscyloskopu LeCroy 804Zi. Wzrost rozdzielczości jest możliwy dzięki stosowaniu łańcucha zbudowanego z elementów opóźniających sterowanych cyfrowo. Prezentowany generator pozwala na generowanie odcinków czasu o określonych przez użytkownika parametrach rozkładu Gausa. (**Wysokorozdzielczy generator odcinków czasu**).*

Keywords: FPGA, time-interval, time-stamp, tapped-delay-line.
Słowa kluczowe: FPGA, odcinek czasu, stempel czasu, wielosegmentowa linia opóźniająca.

Introduction

High resolution TI generators find many applications in science, engineering and industry [1-8]. TI generators may create time-references in many physical experiments, prototyping and in many other different areas such as RADAR and telecommunication systems in general [9,10].

Two different approaches are used to provide TIs (time-delays), namely analogue delay-lines or digital ones. Analogue delay-lines usually use passive components such as RLC circuits, micro-strips or optical fibbers in order to introduce the desired delay for the signal [3,11]. Analogue delay-lines can neither be integrated nor their delay-values are stable in time and independent on the input signal frequency and ambient temperature. The use of digital delay-lines posses many advantages. It allows integrating, obtaining independency on the input-signal frequency and the control that targets most digital systems [1,2].

However, most digital delay-lines, especially those implemented into FPGA structures, posses relatively low resolution and high non-linearity. Higher resolution and smaller non-linearity can be achieved when ASIC (Application-Specific-Integrated-Circuit) technology is used [1,2,12].

This article presents the method of TI generator resolution improvement to the level of single picoseconds. The resolution improvement is obtained by a serial connection of a few DCDEs of different and non-linear characteristics. The proposed TI generator takes advantage of non-ideal parameters (non-linearity and non-repeatability) of TDLs (Tapped-Delay-Lines) implemented in FPGA.

The idea of resolution increase

The idea of precision TI generator consists of using the chain (serial connection) of DCDEs. The single DCDE consists of a TDL with its outputs connected to multiplexer data inputs (fig. 1). The address inputs (Control) of the multiplexer select the TDL output to be passed out. Higher control-value usually chooses paths of higher delay between CLK$_{IN}$ input and CLK$_{OUT}$ output. The characteristic of DCDE is always non-linear and very often may not be even monotonic.

The chain of many DCDEs allows obtaining higher resolution due to mentioned non-linearities. Different real DCDEs may produce slightly different delays for the same control value for two different DCDEs. These differences are getting even smaller when the number of DCDEs increases. Because of non-linearity and non-monotonicity slightly different delay values may also be obtained for different control values in different DCDEs.

Let us suppose there are two four-stage DCDEs of characteristics presented in figure 2. These characteristics are non-linear and monotonic. The average delay change per index change is equal to about 1τ (incremental resolution of single DCDE) for both DCDEs considered separately.
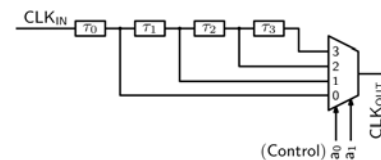

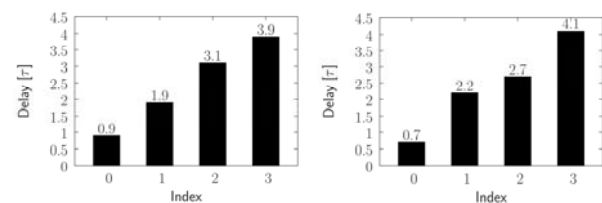Fig.1. The digitally-controlled-delay-element

Fig.2. Exemplary characteristics of two different digitally-controlled-delay-elements

A chain of two or more DCDEs posses higher resolution that single DCDE resolution. Additionally all sorted delay values create the curve that is very similar in shape to the inverse function of Gaussian cumulative distribution (fig. 3). The similarity is higher the larger number of DCDEs is used. It has been experimentally found that four such elements are enough.
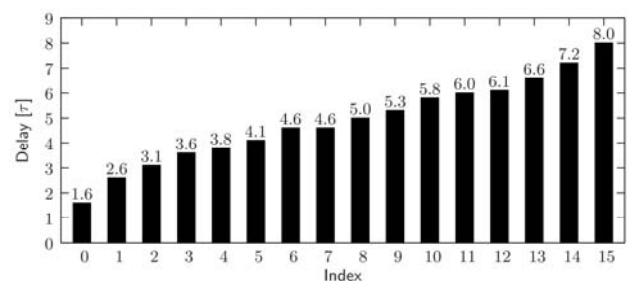

Fig.3. The characteristic obtained for a chain of the two digitally-controlled-delay-elements whose characteristics are presented in figure 2

The process of resolution increase is rather random. As well as the average resolution increases, the number of

paths of the same time-delay value for different control values also increases. Please notice that the characteristic for the chain of two DCDEs presented in figure 3 posses the same value for indexes 6 and 7.

The maximal number of possible paths for the chain of DCDEs is equal to the product of the path numbers of all DCDEs used. However, the total delay generated by the chain of DCDEs is merely equal to the sum of all total delays of all DCDEs used. Assuming that for all DCDEs the average incremental resolution (TDL segment average delay) is equal to τ, the number of segments is equal to n, the number of DCDEs is equal to m and that the minimal path delay is equal to 0, the average incremental resolution of such DCDEs chain is equal to q

$$(1) \qquad q = \frac{n\,\tau m}{n^m} = \tau\,\frac{m}{n^{m-1}}\;.$$

One can see that the average incremental resolution q increases exponentially to the number of DCDEs used m. In fact, this resolution is even better because minimal path delays are larger that 0 – please find that in figure 2, the 0-th bin values are larger than 0. However, the equivalent [13] incremental resolution does not increase exponentially as it will be shown later in this article.

Applying random variables of uniform distribution to DCDE control inputs one can obtain TIs of Gaussian distribution. Controlling the ranges of these random variables allows obtaining TIs of Gaussian distributions of specific standard deviation and average values [1]. The independent random variables of uniform distributions (control values - fig. 1) are easy accessible in computers and do not demand a lot of hardware.
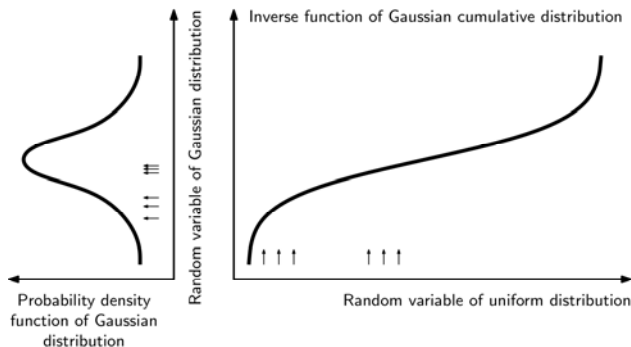

Fig.4. The idea of obtaining random variable of Gaussian distribution by the use of random variable of uniform distribution

Figure 4 shows the process of generation of random variable of Gaussian distribution by the use of random variable of uniform distribution and inverse function of Gaussian-cumulative-distribution. Vertically placed arrows (input argument) represent the random variable of uniform distribution - they are equally distanced. Horizontal arrows, that represent the output values, are being thickened when the Gaussian-cumulative-distribution-inverse-function rises slower and are dispersed when this function rises faster. Consequently the horizontally placed arrows posses Gaussian distribution.

The fact that the delay should have Gaussian distribution results from the central-limit-theorem. The serial connection of several (four or more) DCDEs allows obtaining the delay of Gaussian distribution while each DCDE generates delay of uniform distribution and these delays are independent.

Time-interval generator
This section describes some details of the designed TIG. At the beginning of this section the general idea of

operation is presented and then some chosen blocks of the TIG are discussed more deeply. At the end of this section some details of TIG characteristic measurement and details concerning parameters of Gaussian distribution of generated TIs are presented.

Figure 5 shows the block diagram of the proposed TIG (TIs generator). Generated TI is the sum of TIs produced by the coarse (NT) and the fine (Δt) parts of the TIG. Please, look also shortly at the figure 6 to find the meanings of N, T, and Δt.
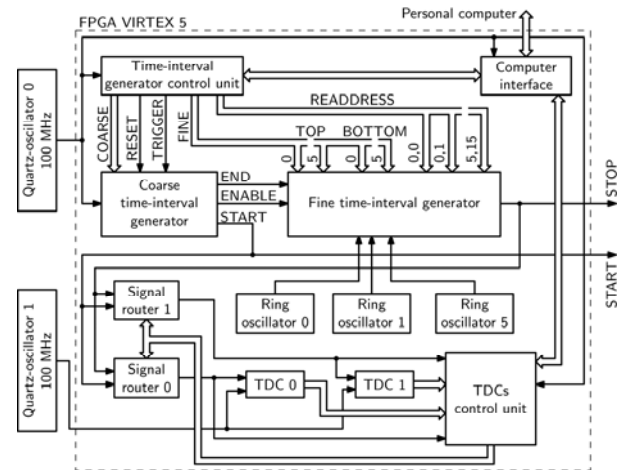

Fig.5. The block diagram of the proposed time-interval generator
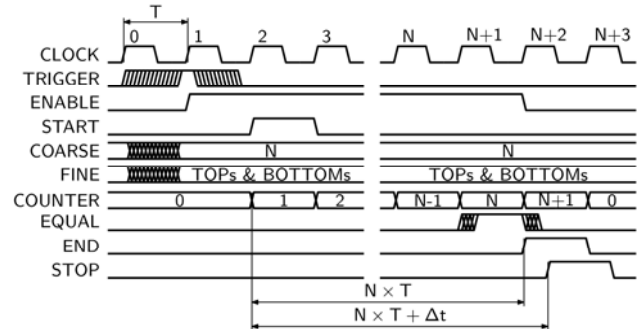

Fig.6. The exemplary timing diagram for the proposed time-interval generator

The COARSE bus (fig. 5) provides the information about the integer number of CLOCK cycles (N) between the START and the END signals (fig. 6). The FINE buses consist of six TOP and BOTTOM pairs - each pair for one DCDE. The TOP and BOTTOM bus states limit the range of randomly generated control values for every DCDE. The READDRESS buses provide the information about the delays order for every DCDE. Readdressing is necessary for assuring the monotonicity of the DCDE characteristic.

The DCDE functionality has been described with the use of VHDL (Very High Speed Integrated Circuits Hardware description Language) language. The single delay-segment has been realized by the LUT1 (Look-Up Table, 1 means one input) component and with the use of 'port map' construction. The average delay introduced by this component is equal to about *320 ps*. The multiplexer has been described behaviorally and no attention was paid to control parasitical delays of its paths. Because of this the original characteristics of DCDEs are not monotonic and that is why the readdressing units are required. In the future designs of TI generators more attention will be devoted to obtain the multiplexer of monotonic characteristic.

The time-interval control-unit is responsible for periodic TRIGGER signal generation. The number of TRIGGER pulses and the distance between them can be regulated. One can set the distance between TRIGGER pulses with the resolution that is equal to the CLOCK (Quartz Oscillator 0) signal period ($10\ ns$).

To start the generation of TI the TRIGGER signal must be high when rising edge of the CLOCK signal appears (fig. 6). After N cycles of the CLOCK signal since the START signal rising edge appeared the END signal is set to high. Both START and STOP signals are 1 the CLOCK signal period wide – there is no possibility of controlling their width.

6 ring-oscillators (fig. 5) are used for the limited (from BOTTOM to TOP) random number generation. All ring-oscillators are asynchronous to the ENABLE signal and posses much higher frequencies (about $400\ MHz$) than the ENABLE signal. Because of this fact the state of the counter incremented by a ring-oscillator can be considered as a random value when read at the ENABLE signal rising edge.
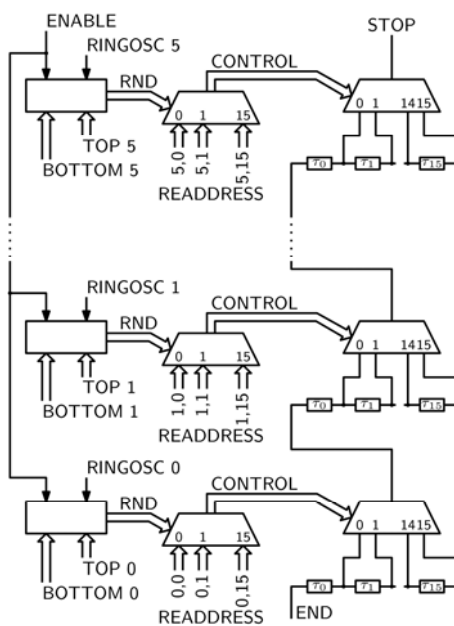

Fig.7. The block-diagram of the fine-part of the designed time-interval-generator

Two TDCs (TDC0 and TDC1) are used for TI generator characteristic measurement [14-20]. Signal routers (Signal router 0 and Signal router 1) can provide either the START and STOP signals respectively to TDC0 and TDC1 inputs or both START and STOP signals (connected by the OR function) simultaneously to both TDCs. In the first case the generated TI can be calculated (many times and then averaged) as the difference between TDC1 and TDC0 results. The sum of these differences can be calculated in the FPGA device on the fly in order to increase the speed of characteristic measurement – there is no need to transmit every difference individually by the Computer interface. It is assumed that all measurement are independent and the standard-deviation of the average-value decreases as $1/\sqrt{n}$, where n is the number of measurements. This assumption can be done because both TDCs are clocked asynchronously (by Quartz oscillator 1) to TIG. And yet, because of the mentioned asynchronicity, the non-linearity of the TDC TDL does not distort the average-value of measured TI, of course in case when number of measurements is sufficient.

The fine-part of TIG consists of 6 identical segments connected in series (fig. 7). Each segment consists of the random-number-generator (the left rectangle), readdressing-unit (the middle multiplexer) and the DCDE (the right multiplexer and the TDL below it). The rising edge of the ENABLE signal generates a new RND state within the range from BOTTOM to TOP states. This causes choosing a new path for the delayed signal. The new path for the delayed signal is chosen sufficiently before the new pulse of the END signal appears (fig. 6) – the passage path of the fine-part of TIG is chosen before the END pulse appears and there is no danger that this path changes during the END pulse is being transferred through it. The RND signal is not connected directly to the DCDE address inputs but the readdressing unit is used. The purpose of the readdressing-unit is to make the characteristic of the fine-part of TIG monotonic in case when it is originally non-monotonic. To use the readdressing-unit one has to measure the characteristic of the particular DCDE and then provide newly calculated order numbers (new order) into READDRESS buses (5,0; 5,1;.. 5,15).

The random number generator used in this work allows for generating random numbers that are in range from BOTTOM to TOP states (fig. 8). The idea of operation is quite simple. The counter CNT is incremented at every rising edge of i-th ring-oscillator (CLK_i). When counter CNT reaches the TOP state then the BOTTOM state is loaded at the next CLK_i rising edge. In this way counter CNT obtains cyclically states from BOTTOM to TOP.

The ENABLE signal posses much larger period than the CLK_i signal. When rising edge of the CLK signal appears then at the nearest falling edge (the CNT state is stable) of the CLK_i signal the state of the CNT counter is registered in REGC. As mentioned before, both clocks are asynchronous, so the registered RND state will be random in range from BOTTOM to TOP.
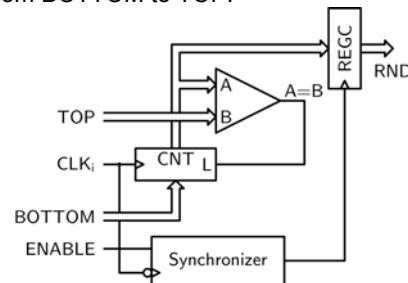

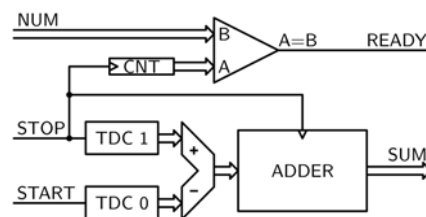Fig.8. The block-diagram of the used random-number-generator

Fig.9. The block-diagram representing the operation in adder-of-differences mode

Generally there are two different possibilities of measuring the characteristic of the TIG implemented in the hardware. The first possibility consists in calculating sum of differences between TSs generated by the START and STOP events (fig. 9). TSs for START and STOP events are measured respectively by the TDC0 and TDC1 (see also fig. 5). These events are represented by rising edges of the START and STOP signals. The ADDER accumulates the differences between TSs obtained for START and STOP events. The CNT counter is incremented every rising edge

of the STOP signal. When the number of accumulations reaches the desired value (NUM) then the READY interrupt is generated and the output of the ADDER can be read by the SUM bus and transmitted to computer.
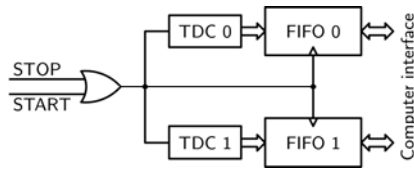

Fig.10. The block-diagram representing the operation in time-stamps mode

In the second mode START and STOP pulses have been connected by the OR function and then they are registered simultaneously by two independent TDCs (fig. 10). This mode allows storing of TSs into memory queues (FIFO0, FIFO1), so later one can calculate TI between START and STOP more precisely because the TDC TDL characteristic can be used for calculations and the TDL non-linearity influence on TS error can be minimized [21]. Each memory block has been built by the use of Block-RAM components and possesses the possibility of storing up to 16384 of 32-bit TSs both for TDC0 and TDC1. Two independently operating TDCs allows increasing the number of measurements so the uncertainty decreases and allows confirming operation correctness of each TDC.

In case when 6 of DCDEs are used and each DCDE posses 16 different paths as many as $16^6=16777216$ different paths are accessible for the whole chain of DCDEs. To reduce the characteristic-measure-time only path-delays for specified vector-control-values are measured – the other ones can be calculated. The knowledge of delays for paths of indexes $(i_1,0,0,0,0,0)$, $(0,i_2,0,0,0,0)$, .., $(0,0,0,0,0,i_6)$, $i_j \in [1,15]$, $j \in [1,6]$ allows obtaining the other ones. The measure-procedure time is reduced $16^6/(16+15\cdot5) \approx 184365$ times in this case. The delay of path of indexes $(i_1, i_2, i_3, i_4, i_5, i_6)$ can be calculated as

$$\tau(i_1,i_2,i_3,i_4,i_5,i_6) = \tau(i_1,0,0,0,0,0) + \tau(0,i_2,0,0,0,0)$$
$$(2) \quad + \tau(0,0,i_3,0,0,0) + \tau(0,0,0,i_4,0,0) + \tau(0,0,0,0,i_5,0) \quad .$$
$$+ \tau(0,0,0,0,0,i_6) - 5\tau(0,0,0,0,0,0)$$

Full characteristics (measured and then completed by calculations – as explained just before) of the TIG are stored in a table of records in a sorted way (with respect to path delays). In fact each, record consists of 6 indexes and the corresponding path delay value. To generate the fine part of the TI one has to find the proper record (path delay value stored in this record is the nearest one to the fine part of the TI that has to be generated) in the table and then pass indexes-values stored in this record as TOP and BOTTOM states (TOP=BOTTOM in this case) (fig. 5 and fig. 6).

TI generator has been designed to be able to generate either precise TIs of specified length or TIs of specified Gaussian distribution. Precise TIs of specified length are generated when DCDE control-values are fixed (TOP buses states are equal to BOTTOM buses states). Whereas TIs of specified Gaussian distribution can be generated by changing control values randomly in specified ranges (from BOTTOM to TOP) by the use of limited random number generator. In this mode standard-deviation and average value are controlled by selecting proper TOP and BOTTOM values. It will be explained in details by examples in the further part of the paper.

Time-interval generator characteristics

Figure 11 shows original (not index-sorted) characteristics for all six DCDEs. These characteristics are non-linear and non-monotonic. To make these characteristics monotonic control inputs of DCDEs have been connected to readdressing-units (fig. 7 – the middle multiplexer) that provides the index conversions. Exemplary the readdressing-unit of the first DCDE should swap indexes 4 and 5, change the index of 12 to 15, change the index 11 to 14 and so on (fig. 11a).
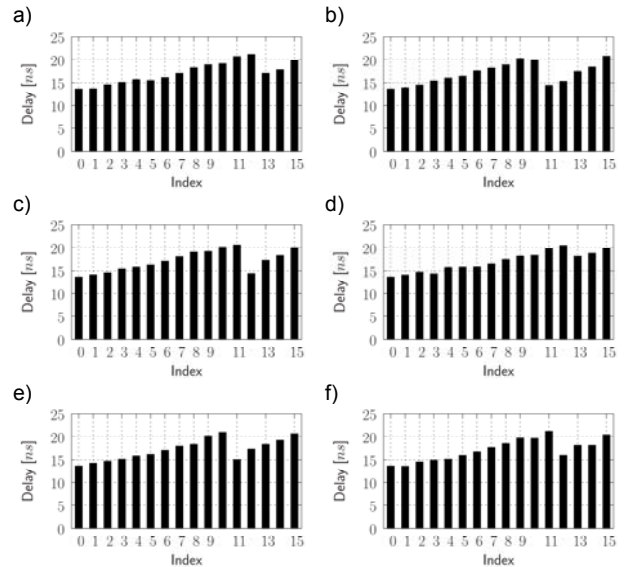

Fig.11. The characteristic of the first (a), second (b), third (c), fourth (d), fifth (e) and sixth (f) digitally-controlled-delay-element

Simulated time-interval histograms

Figure 12 shows delay dependency of the chain of all 6 DCDEs (their characteristics before ordering process are presented in figure 11) on control-values index. The control-values index is just a number assigned to all 6 control-values applied to control inputs (fig. 1, fig. 7) of all DCDEs in such a way that when control-values index increases then DCDEs chain delay also increases.

The control-values indexes in the whole range of delay-values change from 0 to 16777215 (fig. 12). All DCDEs control inputs states change in range from 0 to 15, that can be expressed by (000000-ffffff) (f in hexadecimal notation codes 15). In general notation $(x_1x_2x_3x_4x_5x_6-y_1y_2y_3y_4y_5y_6)$ means here that the control value of the first DCDE changes in range from x_1 to y_1, the control value for the second DCDE changes in range from x_2 to y_2 and so on. This abbreviated notation will be used in the further part of this work for convenience.

In the whole range of control indexes, i.e. from 0 to 2^{24}-1 the characteristic of the fine-part of TIG is very non-linear (fig. 12). However, the incremental resolution is equal to 2.6 fs in average but its maximal value is equal to 290 ps and the equivalent incremental resolution is equal to 30.4 ps. However, in the relatively wide and well-defined range of generated time-delays, when control indexes change from 10^3 to 2^{24}-1-10^3, the maximal incremental resolution value is not larger than 5 ps, and its equivalent value is equal to 1 ps. This restriction has limited the range of time-delays generated by the fine-part of TIG from the original range of from 13.6 ns to 57.3 ns to the range of from 16.1 ns to 53.8 ns. When the control indexes have been limited to the range of from 2×10^6 to 2^{24}-1-2×10^6, then both the maximal value of incremental resolution and equivalent incremental resolution value decreased to 1 ps. This control-index

restriction limited the time-delays generated by the fine-part of TIG to the range from *27.7 ns* to *41 ns*. The width of this range is slightly above *10 ns*, and it is enough. The range can be successfully extended by the coarse-part of TI generator that generates TI with resolution of *10 ns* in the range that is only limited by the capacity of the counter. Of course FPGA structure temperature fluctuations as well as supply voltage noise and disturbances cause that the single TI posses much greater uncertainty that this resolution. All the measurements have been carried out for relatively constant (*±1 °C*) ambient temperature. Even though neither structure temperature stabilization nor voltage regulation were applied, the average value of generated TIs of constant length could be controlled with picoseconds precision (fig. 16). To obtain the dependency presented in figure 12 only *16+5·15* measuring series have been carried out and averaged (each measuring series consists of 2^{24} TIs), then the equation 2 has been applied to complete the lacking information. The fact that the characteristic of the fine-part is non-linear and is becoming even more non-linear when the number of DCDE elements increases (see also figures 2 and 3) is meaningless until the maximum value of incremental resolution does not exceed the desired TIG resolution in the range that is larger or equal to the standard-clock period that cycles the coarse-part of TIG.
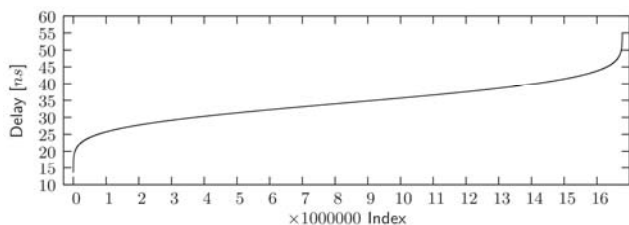

Fig.12. Digitally-controlled-delay-elements delay dependency on control-values index (all control-values change in the full range)
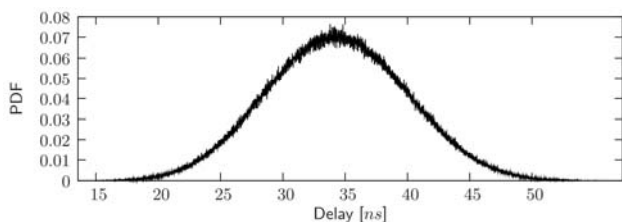

Fig.13. Probability-density-function of time-intervals obtained from the delay-dependency on control-values index presented in figure 12 in the way presented in figure 4

Figure 13 shows the simulated TIs histogram obtained from the delay dependency on control-vaclues index presented in figure 12. The method of obtaining this TIs histogram is explained in figure 4. The obtained distribution is sufficiently similar to the Gaussian one. Here the control-values have been changing in full range, i.e. *(000000-ffffff)*. By changing control-values in limited ranges one can obtain Gaussian distribution of desired average-value and standard-deviation.

Figure 14 shows DCDEs delay dependencies on control-values index (a) and PDFs of TIs (b) in case when DCDEs control-values have been limited. The Limit-values have been selected in such a way that the product of corresponding index states numbers is constant for all cases (cases from *a* to *f* of figure 14). For example (fig. 14, case a) when control-values change in range *(000000-333333)*, the number of states for every DCDE is equal to *3-0+1=4*. The number of states for the whole DCDEs chain is equal to $4^6=4096$. One can easily check that the numbers of

states for all other cases, i.e. b,c,d,e,f of figure 14, are equal to each other. This number of states determines the standard-deviation of TIs Gaussian distribution. Please notice (fig. 14b) that all PDFs posses approximately equal to each other standard-deviation.
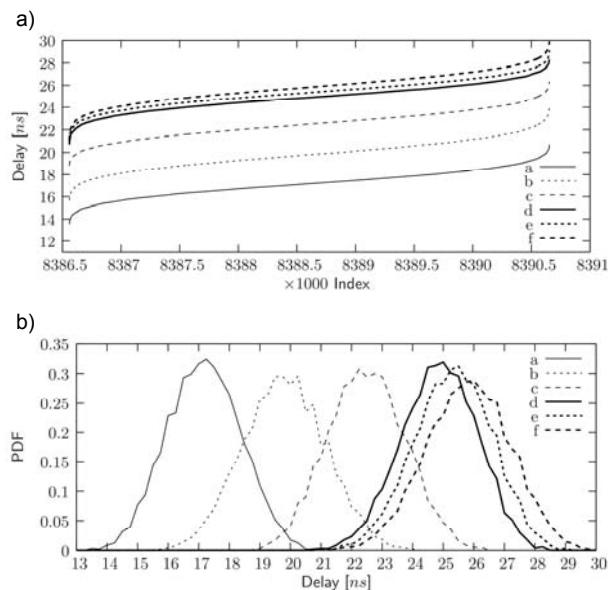

Fig.14. Digitally-controlled-delay-elements (a) delay dependencies on control-values index, (b) probability density functions, in case of constant standard deviation and variable average value of Gaussian distribution; Control values change in ranges; a − *(000000-333333)*, b − *(111111-444444)*, c − *(222222-555555)*, d − *(333333-666666)*, e − *(333334-666667)* and f − *(333344-666677)*.
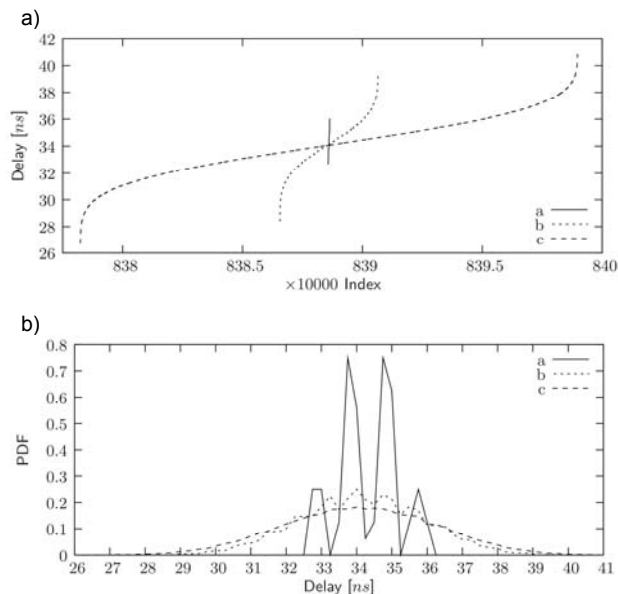

Fig.15. Digitally-controlled-delay-elements (a) delay dependencies on control-values index, (b) probability density functions, in case of variable standard deviation and constant average value of Gaussian distribution; Control values change in ranges; a − *(777777-888888)*, b − *(666666-999999)* and c − *(555566-aaaa99)*.

The sum of these limits determines the average value of TIs Gaussian distribution. When the sum of these limit-values increases, the average value of TIs Gaussian distribution also increases. In case a (fig. 14) this sum is equal to *6·(0+3)=18*, for all other cases (case from b to f) these sums are equal respectively to *6·5=30*, *6·7=42*, *6·9=54*, *5·9+11=56* and *4·9+2·11=58*.

Figure 15 shows cases when the sums of limit-values are constant. For all cases presented in figure 15 these sums are equal to *15*. This means that all TIs PDFs posses the same average value (all DCDEs delay dependencies (fig. 15a) crosses at the same point). However, in all these cases the product of corresponding index states numbers differs. These products determine the standard deviations of TIs PDFs. For all cases of figure 15 these products are equal respectively to $2^6=64$, $4^6=4096$ and $6^4 4^2=20736$. Unfortunately this relation, i.e. dependency of PDF standard-deviation on the product of DCDEs state numbers, is very non-linear and unpredictable. To generate TIs of specified standard-deviation one has to use look-up-tables rather than simple mathematical formula.

Time-intervals of specified length

Figure 16 shows ten different histograms of TIs of specified lengths. TIs of specified length are generated in case when top and bottom limit-values for all DCDEs are equal to each other. In this case standard deviations of generated TIs obtain the smallest possible values. Nominally time-delays generated by all DCDEs are constant, all time fluctuations visible in TIs histograms (fig. 16) are causes by imperfections of TIG and imperfections of oscilloscope (the LeCroy 804Zi). The nominal (set by the use of the DCDEs characteristics) average-values of five upper TIs (fig. 16a) and five lower (fig. 16b) TIs intentionally differ by *10 ps*. Results show that the measured TIs average values differ from the nominal values by less than *2 ps* on average. The corresponding TIs histograms average values differences differ from *10 ps* by less than *1 ps* on average. These results show that it is possible to generate TIs with average resolution of single picoseconds.
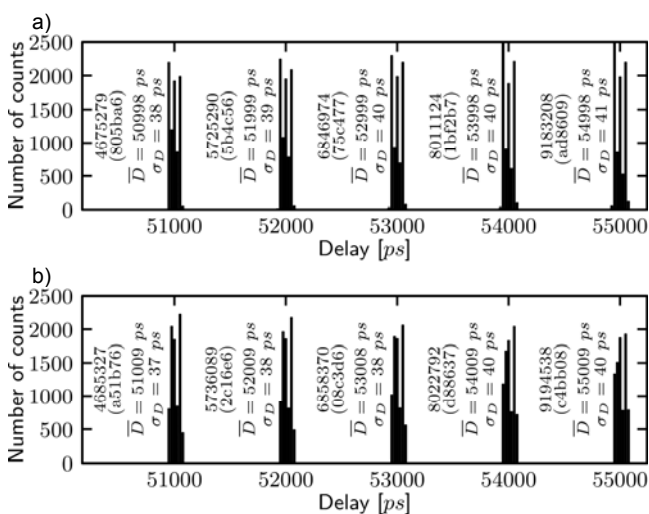

Fig.16. Histograms of time-intervals of specified length obtained for ten different control values. Bottom time-interval histograms (b) are intentionally shifted (delayed) by *10 ps* relatively to top ones (a). Control-values are placed in parenthesis, control-values indexes are placed just above them.

In fact the time-noise visible in histograms was also produced by the LeCroy 804Zi oscilloscope and was not negligible. When both probes of the oscilloscope were shortened then TIs of Gaussian distribution of standard deviation of about *20 ps* were measured. The largest standard-deviation of all 10 peaks is equal to *40 ps*. Removing the oscilloscope influence, one can find that the standard deviation of generated TIs is less than *35 ps* ($40^2-20^2 \approx 35^2$).

Figure 16 also shows how high is the resolution of TI generator. Taking into account two first peaks of indexes *4675279* and *5725290* one can notice that there are *1050011* different possible TIs to be generated in time-range from about *51 ns* to *52 ns*. This means that the average resolution in that range is equal to about *0.95 fs* per index. Even better resolution of about *0.85 fs* can be obtained in range from *54 ns* to *55 ns*. Similar conclusions can be obtained when analyzing figure 12. Of course these are only entirely theoretical considerations. In Practice a few different sets of control values can generate very similar or even equal to each other time-delays and some delays can be much larger than its average value. More adequate than the average value of the incremental resolution would be its equivalent value. For the range mentioned in this paragraph the equivalent value of the incremental resolution is equal to *290 fs*. The maximal value of the incremental resolution in this range was equal to *870 fs*.

The designed and constructed TIG would be able theoretically to generate TIs of resolution even better than *1 fs*. However, the measurements show that this resolution is much worse and is equal to about *1 ps* in case when average value of generated TIs is taken into account. Generated TIs posses relatively high uncertainty of about *35 ps*. It is suspected that the standard-clock short-term jitter is responsible for such high uncertainty. This suspicion arisen from the fact that TI histograms between consecutive rising edges possessed 2 or 3 maximums (fig. 12) independently on the time-delay generated by the fine-part of the TIG. TI histogram introduced by the fine-part of the TIG would rather posses the Gaussian distribution. If the fine-part of the TIG introduces higher uncertainty that the standard-clock short-term jitter these maximums would not be visible.

Time-intervals of specified Gaussian distribution

Figure 17 shows three TIs histograms measured in case when limit-values have been selected in such a way that standard deviations σ_t are all equal to *1750 ps*, and average-values t are equal respectively to *50 ns*, *55 ns* and *60 ns* according to the model implemented in control-software. This model uses the characteristics (after ordering process) presented in figure 11. Generated TIs histograms posses very similar standard-deviations and average-values to the set (nominal) by control-software values. This high level of equality of these parameters of generated TIs has been achieved by implementing an algorithm that is looking for the best match by the use of software model that bases on DCDEs characteristics. Please find out by analyzing the caption of figure 17 that the products of corresponding index states numbers are not equal to each other as it was in case presented in figure 14.

On contrary to figure 17, figure 18 presents TIs histograms obtained in case when limit-values have been selected in such a way that the average-values of generated TIs are constant ($t=50$ ns) and desired standard deviations are equal respectively to *500 ps*, *1 ns*, *2 ns*. Similarly as it was in the previous case limit-values have been calculated by the just mentioned algorithm implemented in the control-software. By analyzing the caption of figure 18 one can conclude that sums of limit-values are not constant as it was in case of figure 15. The reason of this difference is the same as in the previous paragraph. These parameters have been modified by software matching algorithm that uses DCDEs characteristics.

There are some imperfections in standard-deviation values, and average-values and shapes of the histograms. However the correlation between set parameters and obtained Gaussian histogram parameters are really

impressive. One can notice that when the standard deviation of the generated TIs is smaller than or equal to *1 ns* (fig. 18a,b), then shapes of the histograms are abnormal. Instead of one smooth Gaussian shape several individual peaks are visible. This is caused by the small number of possible states of the fine-part of TI generator that may be used to generate TI within the desired Gaussian shape limited by standard deviation value. Please find in the caption of the figure 18 that in case (a) the number of different states is only equal to *8*. The number of different states in case (b) is equal to *144* while a such number in case (c) is equal to *19600*. When the standard deviation of generated TIs increases then the number of possible states of fine-part of TIG also increases (unfortunately this is not a linear dependence). Increasing the number of DCDEs would help to condense larger number of different states in the limited range.
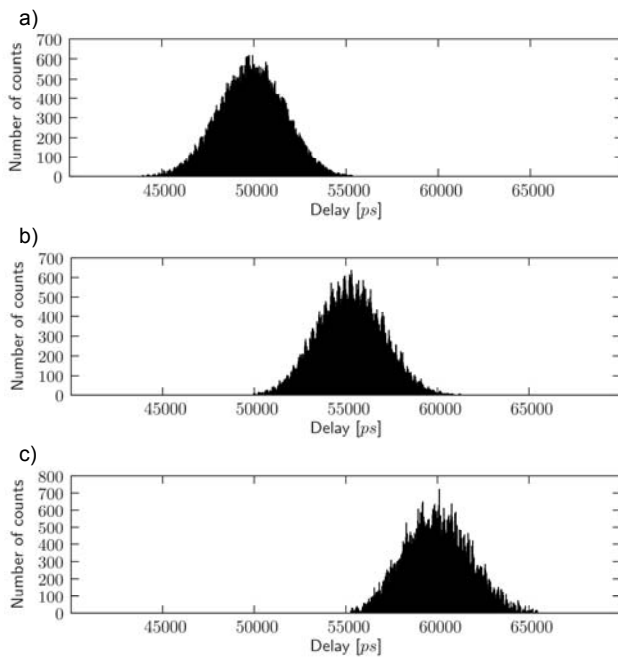
a)

b)

c)

Fig.17. Time-interval histograms of specified Gaussian distribution with constant standard deviation ($\sigma_t=1750~ps$) and variable average values ((a) *t=50 ns*, (b) *55 ns*, (c) *60 ns*). Measured standard deviations are equal to (a) *1739 ps*, (b) *1747 ps*, (c) *1744 ps*. Measured average values are equal to (a) *49.87 ns*, (b) *55.23 ns*, (c) *59.99 ns*. Control delay values are in ranges (a) *(139156-57d589)*, (b) *(969165-bad4a9)*, (c) *(aa8559-eea99a)*.

The TIG fine-part range of generated TIs in this mode depends strongly on their standard-deviation. When standard deviation is higher, the range of generated TIs is smaller. Figure 13 allows estimating maximum value of TIs standard-deviation σ_t dependency on its length *t* and vice versa. This rule is quite simple.

The generated TI length *t* can vary (in both directions) from the Gauss center position (about *35 ns*) as much as its threefold standard-deviation $3\sigma_t$ differs from the threefold standard deviation of the Gauss presented in figure 13 (*5 ns*). For example when *t=30 ns* (TI generated by fine part of the TIG) then maximal σ_t is equal to about *3.33 ns*, and when *t=35 ns* then its standard-deviation can not be greater than *5 ns*. When standard-deviation would be equal to *1.5 ns* then TI could be generated in range from *24 ns* to *44 ns*, but when $\sigma_t=2~ns$ generated TIs average value can be in range *26 ns* to *42 ns*.

a)

b)

c)
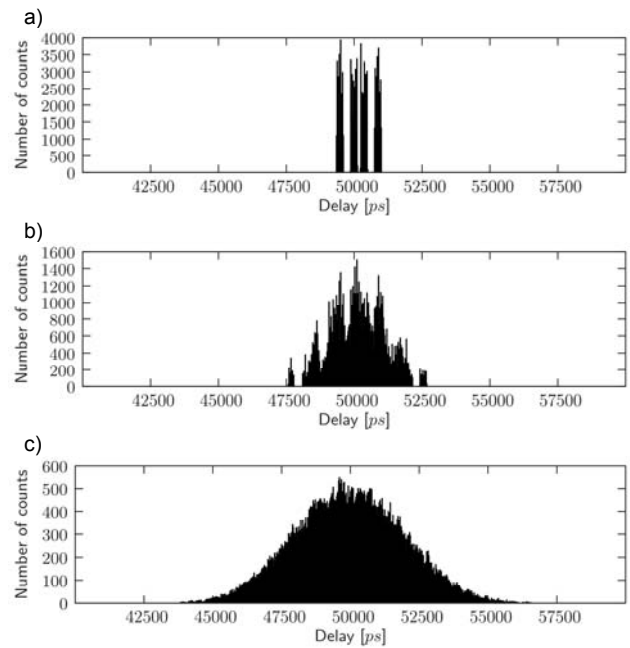

Fig.18. Time-interval histograms of specified Gaussian distribution with constant average value (*t=50 ns*) and variable standard deviations ((a) $\sigma_t=500~ps$, (b) *1 ns*, (c) *2 ns*). Measured standard deviations are equal to (a) *517 ps*, (b) *1001 ps*, (c) 1957 ps. Measured average values are equal to (a) *50.17 ns*, (b) *50.13 ns*, (c) 49.97 ns. Control delay values are in ranges (a) *(25b368-35c378)*, (b) *(24a367-36c478)*, (c) *(029156-68c599)*.

In this case, when the range is extended by the coarse part of the TIG of period *10 ns*, the TIs generated by the fine-part of TIG should be in range from *0* to *10 ns*. This means that maximum standard-deviation of any TIs set can maximally be equal to about *3.33 ns*.

Conclusions

The method of resolution improvement and hardware Gaussian distribution generation appeared to be very useful. TI generator can generate TIs of average-value with resolution of *1 ps* in practically unlimited range extended by its coarse-part. The standard-deviation of generated TIs can be adjusted in range from about *35 ps* to about *3.33 ns*. The implemented in the control software algorithm allows for matching DCDEs control-values and obtaining TIs of desired parameters. Unfortunately for smaller standard deviation values (when $\sigma_t \le 1ns$) of generated TIs the shape of obtained TIs histogram does not reflect the Gaussian shape. The solution of this problem would consist in increasing the number of DCDEs.

Author: Dariusz CHABERSKI[1]
Nicolaus Copernicus University, Faculty of Physics, Astronomy and Informatics, 87-100 Toruń, Poland (1)

REFERENCES
[1] Arkani M., Khalafi H., Vosoughi N., A Flexible Multichannel Digital Random Pulse Generator Based on FPGA, *World Journal of Nuclear Science and Technology*, 3 (2013), n. 4, 109-116
[2] Xu Rugi, Nguyen Cam, A high precision close-loop programmable CMOS delay generator for UWB and time domain RF applications, *Microwave and Optical Technology Letters*, 53 (2011), n. 2, 390-392
[3] Zhang J., Cheung S.W., Yuk T.I., A Compact and UWB Time-delay Line Inspired by CRLH TL Unit Cell, *The 2010 IEEE Region 10 International Conference, Fukuoka, Japan*, 2010, 868-872

[4] Otsuji T., Narumi N., A 3-ns Range, 8-ps Resolution, Timing Generator LSI Utilizing Si Bipolar Gate Array, *IEEE Journal of Solid-State Circuits*, 26 (1991), n. 5, 806-811

[5] Yao Y., Wang Z., Lu H., Chen L., Jin G., Design of time interval generator based on hybrid counting method, *Nuclear Instruments in Physics Research A*, 832 (2016), 103-107

[6] Otsuji T., Narumi N., A 10-ps Resolution, Process-Insensitive Timing Generator IC, *IEEE Journal of Solid-State Circuits*, 24 (1989), n. 5, 1412-1418

[7] Kwiatkowski P., Różyc K., Sawicki M., Jachna Z., Szplet R., 5 ps jitter programmable time interval/frequency generator, *Metrology and Measurement Systems*, 24 (2017), n. 1, 57-68

[8] Chen P., Chen P.-Y., Lai J.-S., Chen Y.-J., FPGA Vernier Digital-to-Time Converter With 1.58 ps Resolution and 59.3 Minutes Operation Range, *IEEE Trans. Circuits Syst. I, Reg. Papers*, 57 (2010), n. 6, 1134-1142

[9] Abdel-Aal R. E., A Programmable Gaussian Random Pulse Generator for Automated Performance Measurements, *Nuclear Instruments and Methods in Physics Research Section A: Accelerators, Spectrometers, Detectors and Associated Equipment*, 276 (1989), n. 3, 573-576

[10] Tang Wenjia, Kim Hongjoon, Compact, tunable large group delay line, *Wireless and Microwave Technology Conference, WAMICON '09. IEEE 10th Annual, Florida*, 2009, 1-3

[11] Zhang J., Zhu Q., Jiang Q., Xu S.J., Design of time delay lines with periodic microstrip line and composite right/left-handed transmission line, *Microwave and Optical Technology Letters*, 51 (2009), n. 7, 1679-1682

[12] Kim Choul-Young, Yang Jaemo, Kim Dong-Wook, Hong Songcheol, A K-Band CMOS Voltage Controlled Delay Line Based on an Artificial Left-Handed Transmission Line, *IEEE Microwave and Wireless Components Letters*, 18 (2008), n. 18, 731-733

[13] Wu J., Uneven Bin Width Digitization and a Timing Calibration Method Using Cascaded PLL, *FERMILAB-CONF-14-140-E*

[14] Zieliński M., Chaberski D., Kowalski M., Frankowski R., Grzelak S., High-resolution time-interval measuring system implemented in single FPGA device, *Measurement*, 35 (2004), n. 3, 311-317

[15] Kalisz J., Review of methods for time interval measurements with picosecond resolution, *Metrologia*, 41 (2004), n. 1, 17-32

[16] Chaberski D., Time-to-digital-converter based on multiple-tapped-delay-line, *Measurement*, 89 (2016), 87-96

[17] Giordano R., Ameli F., Bifulco P., Bocci V., Cadeddu S., Izzo V., Lai A., Mastroianni S., Aloisio. A., High-Resolution Synthesizable Digitally-Controlled Delay Lines, *IEEE Transactions on Nuclear Science*, 62 (2015), n. 6, 3163-3171

[18] Szplet R., Sondej D., Grzęda G., High-Precision Time Digitizer Based on Multiedge Coding in Independent Coding Lines, *IEEE Transactions on Instrumentation and Measurement*, 65 (2016), n. 8, 1884-1894

[19] Szplet R., Kwiatkowski P., Jachna Z., Różyc K., An Eight-Channel 4.5-ps Precision Timestamps-Based Time Interval Counter in FPGA Chip, *IEEE Transactions on Instrumentation and Measurement*, 65 (2016), n. 9, 2088-2100

[20] Li J., Zheng Z., Liu M., Wu S., Large Dynamic Range Accurate Digitally Programmable Delay Line with 250-ps Resolution, *International Conference on Signal Processing*, Beijing, China, 16-20 Nov. 2006

[21] Chaberski D., Zieliński M., Grzelak S., The new method of calculation sum and difference histogram for quantized data, *Measurement*, 42 (2009), 1388-1394